



NIST Technical Note
NIST TN 2025r1

Intelligent Building Agents Laboratory

Air System Design

Dr. Amanda J. Pertzborn
Dr. Daniel A. Veronica
Glen A. Glaeser

This publication is available free of charge from:
<https://doi.org/10.6028/NIST.TN.2025r1>

**NIST Technical Note
NIST TN 2025r1**

Intelligent Building Agents Laboratory

Air System Design

Dr. Amanda J. Pertzborn
*Building Energy and Environment Division
Mechanical Systems and Controls
Engineering Laboratory*

Dr. Daniel A. Veronica
*Building Energy and Environment Division
Mechanical Systems and Controls
Engineering Laboratory*

Glen A. Glaeser
*Building Energy and Environment Division
Mechanical Systems and Controls
Engineering Laboratory*

This publication is available free of charge from:
<https://doi.org/10.6028/NIST.TN.2025r1>

January 2024



U.S. Department of Commerce
Gina M. Raimondo, Secretary

National Institute of Standards and Technology
Laurie E. Locascio, NIST Director and Under Secretary of Commerce for Standards and Technology

NIST TN 2025r1
January 2024

Certain equipment, instruments, software, or materials, commercial or non-commercial, are identified in this paper in order to specify the experimental procedure adequately. Such identification does not imply recommendation or endorsement of any product or service by NIST, nor does it imply that the materials or equipment identified are necessarily the best available for the purpose.

NIST Technical Series Policies

[Copyright, Use, and Licensing Statements](#)

[NIST Technical Series Publication Identifier Syntax](#)

Publication History

Approved by the NIST Editorial Review Board on 2024-01-18

Supersedes NIST Technical Note 2025 (September 2018) <https://doi.org/10.6028/NIST.TN.2025>

How to Cite this NIST Technical Series Publication

Pertzborn AJ, Veronica DA, Glaeser GA (2024) Intelligent Building Agents Laboratory: Air System Design. (National Institute of Standards and Technology, Gaithersburg, MD), NIST Technical Note (TN) NIST TN 2025r1.

<https://doi.org/10.6028/NIST.TN.2025r1>

Author ORCID iDs

Amanda J. Pertzborn: 0000-0002-1473-7500

Daniel A. Veronica: 0009-0003-8009-1547

Glen A. Glaeser: 0009-0007-9383-5224

Contact Information

amanda.pertzborn@nist.gov

Abstract

The National Institute of Standards and Technology has constructed the Intelligent Building Agents Laboratory (IBAL) to demonstrate the potential for distributed, intelligent software agents to optimize the control of heating, ventilation, and air-conditioning systems in commercial buildings. The goal of the optimization is to improve the economic and energy performance of building systems while maintaining occupant comfort. This paper describes the design of, and the equipment in, the airside system of the IBAL.

Keywords

HVAC; intelligent agent; air system

Table of Contents

1. Introduction	1
2. Description of the IBAL	4
2.1. Overview.....	4
2.2. Outdoor Air Unit.....	6
2.3. Air Handling Units.....	9
2.4. Variable Air Volume Units.....	11
2.5. Zone Simulators.....	13
2.6. Exhaust Fans.....	18
2.7. Data Collection and Operation.....	18
3. Measurement Uncertainty Calculations	19
3.1. Overview.....	19
3.2. Uncertainty of Calibration Curve Fit.....	20
3.3. Pressure Transducers.....	21
3.4. Airflow Sensors.....	23
3.5. Relative Humidity Sensors.....	24
4. Summary and Future Work	25
5. References	26
Appendix A. List of Symbols, Abbreviations, and Acronyms	27
Appendix B. Sensor Information	29
Appendix C. Change Log	32

List of Tables

Table 1. Specifications for the components in the OAU.	6
Table 2. Specifications for the components in the AHU.	9
Table 3. Loads for Case 1: open office space.....	15
Table 4. Loads for Case 2: conference room.	16
Table 5. Specifications for the components in the ZSs.	16
Table 6. Specifications for the exhaust fans.....	18
Table 7. Uncertainties of temperature, voltage, and current measurements of DAQ hardware. ...	20
Table 8. Air pressure transducer uncertainty results.....	22
Table 9. Measurement uncertainty of airflow sensors.....	23
Table 10. Conversion factors for airflow sensors.	23
Table 11. Measurement uncertainty and calibration fit for RH sensors.	24
Table 12. Summary of sensors in the air system in the IBAL.....	29
Table 13. Calibration data for pressure transducers.	30
Table 14. Calibration data for relative humidity sensors.....	31

List of Figures

Fig. 1. Picture of most of the air system.	3
Fig. 2. Picture of most of the hydronic system.	3
Fig. 3. Schematic of the IBAL air system.	5
Fig. 4. Legend for the component schematics.	7
Fig. 5. Outdoor air unit (OAU).	8
Fig. 6. Picture of the OAU. Air is drawn in from the lower left, exits the OAU on the upper left of the unit, and goes to the AHUs at the right (not shown).	9
Fig. 7. Air Handling Units (AHUs). See Fig. 4 for the legend.	10
Fig. 8. AHU2 (top) and AHU1 (bottom). The OAU is on the upper mezzanine at the far left of the picture and the VAVs, not shown, are to the right.	11
Fig. 9. Variable air volume boxes (VAV). See Fig. 4 for the legend.	12
Fig. 10. Picture of the VAVs. The AHUs are to the left and the ZSs are to the right.	13
Fig. 11. Zone simulators (ZS). See Fig. 4 for the legend.	14
Fig. 12. Picture of the four ZSs. The VAVs are at the left.	15
Fig. 13. The black tanks hold water for the thermal mass coils in the zone simulators. Above the tanks are the red circulating pumps that move the water through the TMCs. The flow rate is determined by manually setting a valve.	17
Fig. 14. Picture of the air pressure calibration setup. The precision pressure controller is at the far left and two pressure transducers (the gray boxes) are visible.	22

1. Introduction

Achieving national goals of net zero energy buildings requires substantial reduction in the energy consumption of commercial building systems. In 2017, commercial buildings consumed 18 % of the total energy consumed in the U.S. [1]. Although significant progress has been made in the integration of building control systems through the development of standard communication protocols, such as BACnet and BACnet/IP, little progress has been made in making them “intelligent” about optimizing building system-level performance. The focus of this project is to demonstrate the potential for distributed, intelligent software agents to perform this optimization. That focus required designing and building a research infrastructure suitable for development and testing of advanced agent-based optimization techniques to improve the energy and comfort performance of heating, ventilating, and air conditioning (HVAC) systems in buildings.

An intelligent agent can take many forms, but the basic concept is that it acquires information about the state of the system, makes an optimal or near-optimal control decision, and communicates that decision to another agent or to an actuator that executes the decision. The agent can represent a piece of HVAC equipment such as an air-handling unit (AHU) and learn how that AHU operates over time to produce an optimal or near-optimal operating point given the current or forecast system conditions. An HVAC system would contain multiple agents that communicate to make choreographed control decisions that lead to optimal or near-optimal operation of the overall system. In this way the decision-making process is distributed.

Kelly and Bushby [2] completed a feasibility study to determine if intelligent agent technology could lead to significant savings in HVAC energy consumption. Their study was comprised of 17 agents:

- 8 – VAV (variable air volume) agents
- 2 – AHU agents
- 2 – Chiller agents
- 2 – Cooling tower agents
- 1 – Agent to coordinate the actions of the other agents
- 1 – Agent to quantify the operating cost of the system
- 1 – Agent to control the simulation

To simulate the learning that an agent would have to do in the real world to understand how a given piece of equipment operates, models of each HVAC component were developed and used to provide data to the agent under a variety of conditions. Regression models were developed based on the data and these models were incorporated into the agents to predict equipment performance. With the agents now capable of estimating the

performance of their equipment, the next step was to develop a method to optimize system performance.

Kelly and Bushby tested two methods, a simple optimization method (SOM) and an advanced optimization method (AOM). Only the SOM will be presented here because the AOM did not lead to a significant increase in savings relative to SOM. In SOM, the HVAC agents take turns optimizing the operation of their equipment. The optimal operation of one piece of equipment often conflicts with the optimal operation of another piece of equipment. For example, the AHU may have optimal performance when the chiller provides it with water at 1.7 °C (35 °F), but the chiller may have better performance producing water at 12.8 °C (55 °F). In each time step, one agent determines how it would like to operate its equipment, calculates the cost of that operation, and communicates with the other agents to determine what the impact of that operation is on the other equipment in the system and the overall system cost. The agent can then decide if, given the overall impact on the system, it should change its set point as proposed. In the next time step, a different agent leads this process.

Kelly and Bushby [2] showed that, in a simulation of a single day of operation, the cost savings over a reference case without optimization was 21 %. Although the authors note that these savings are dependent on the details of the reference case, this proof-of-concept study was promising enough to justify the construction of a laboratory to test the concept using actual HVAC equipment. The Intelligent Building Agents Laboratory (IBAL) is the culmination of that effort. The IBAL contains an air system able to emulate those typically found in commercial buildings and a hydronic system able to emulate a variety of designs typical of their plants. The IBAL is capable of representing a building having a modern, efficient HVAC system, or a building constrained by an older, more obsolescent design.

The air system is located on a mezzanine (see Fig. 1) and the hydronic system is located underneath the mezzanine (see Fig. 2). There is an AHU dedicated to conditioning outdoor air to produce repeatable test conditions and zone simulators to emulate building loads. All of the equipment are monitored and controlled from a central data acquisition (DAQ) system. This technical note will describe the design and construction of the air system; Ref. [3] described the hydronic system in detail.



Fig. 1. Picture of most of the air system.

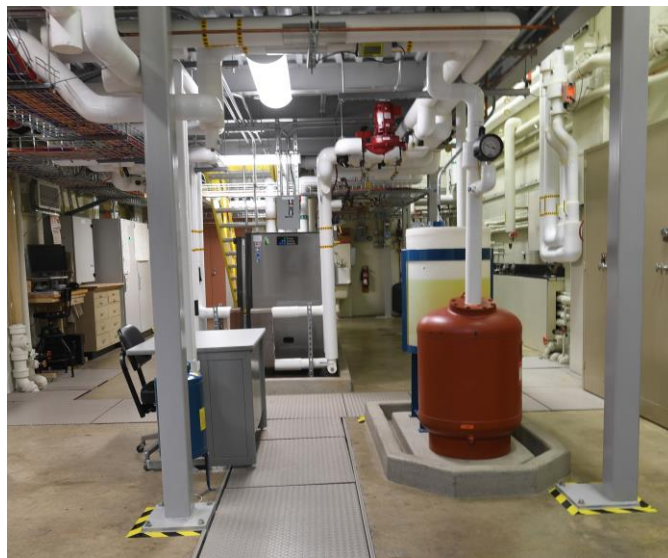


Fig. 2. Picture of most of the hydronic system.

2. Description of the IBAL

The purpose of the IBAL is to emulate a small office building in terms of the complexity and the type of HVAC systems and equipment that would typically be present. Since the primary use of the facility is conducting consistently controlled experiments that characterize the performance of a wide variety of intelligent control algorithms, system design decisions and equipment selections were made to allow as many control options as possible. This section will describe the mechanical design of the air system of the IBAL in detail.

2.1. Overview

The IBAL contains the following equipment:

- Air system
 - 1 – Outdoor air unit (see Sec. 2.2)
 - 2 – Air handling units (see Sec. 2.3)
 - 4 – Variable air volume units (see Sec. 2.4)
 - 4 – Zone simulators (see Sec. 2.5)
 - 2 – Exhaust fans (see Sec. 2.6)
- Hydronic system
 - 2 – Chillers
 - 1 – Thermal storage tank
 - 3 – Heat exchangers

This technical note will describe the air system, shown in Fig. 3. Later sections will discuss and show each component in more detail. At the far left is the outdoor air unit (OAU). This component conditions the actual outdoor air to provide the simulated outdoor air conditions for each test, which allows the same test to be repeated on different days. The OAU provides simulated outdoor air to two AHUs, which condition the simulated outdoor and return air to meet the needs of the four zones. The cooling coils in the AHUs use a 30 % propylene glycol (PG) mixture from the chillers to cool and dehumidify the air. The system is nominally designed so that a single AHU serves two zones, and the variable air volume (VAV) units are used to modify the air temperature and/or flow rate to meet the needs of the individual zone. However, dampers D9 and D12 (see Fig. 3) can be opened to allow one AHU to serve more than two zones. The four zone simulators (ZSs) provide a load for the system and the exhaust fans (EXFs) are used to reject air outside of the building.

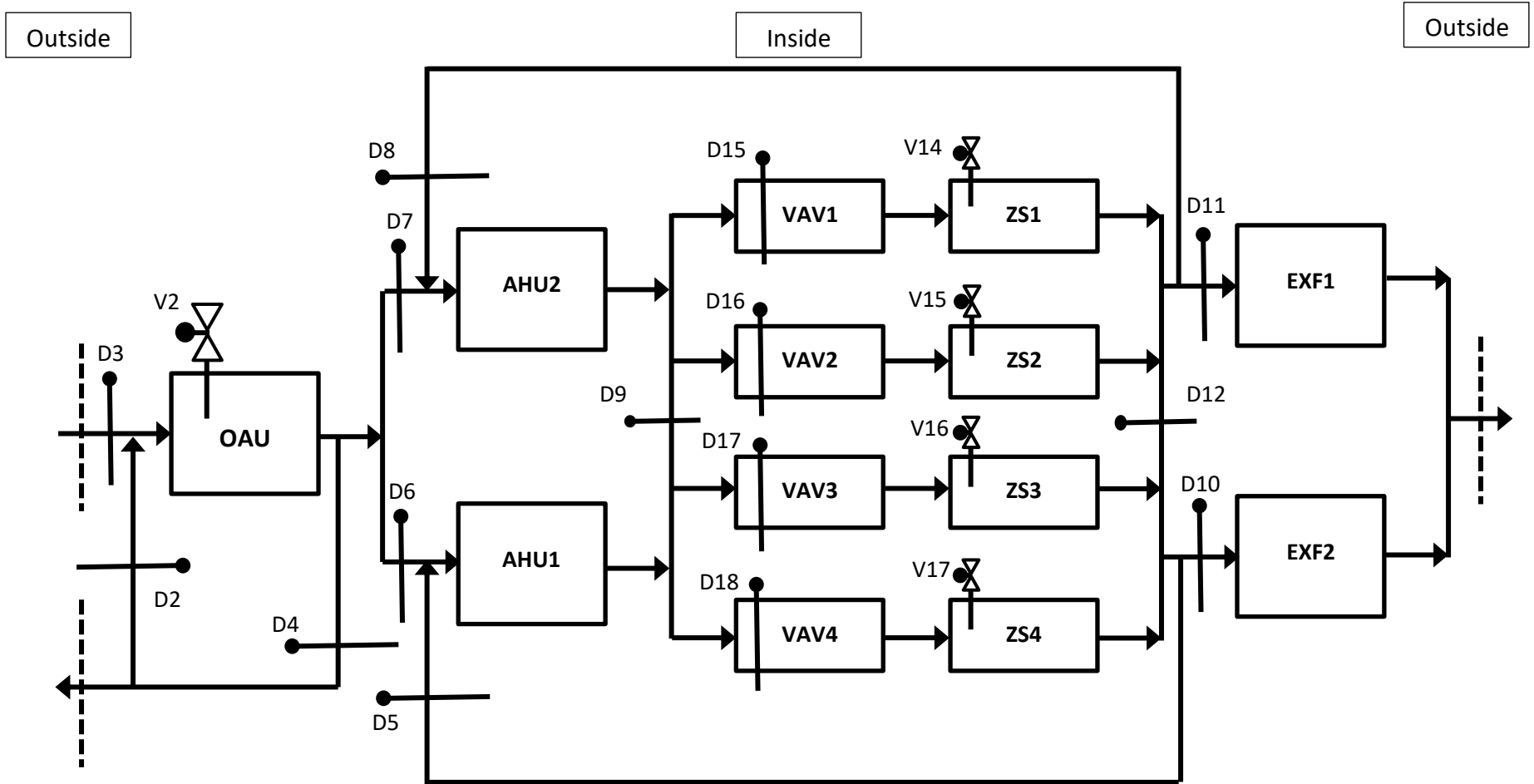


Fig. 3. Schematic of the IBAL air system.

2.2. Outdoor Air Unit

The OAU conditions outside air to simulate weather conditions for laboratory testing. The independent regulation of both the temperature and humidity of the air being supplied by the OAU is essential to the creation of relevant and repeatable test scenarios. The appropriate design for the OAU is thus one following the concept of a “single-zone” air system as described by Lorsch in [4]; here the single “zone” is a continual flow of air supplied as if drawn in from outside at a specified “outdoor” condition. Figure 4 is the legend for Fig. 5, which shows the components of the OAU and the installed sensors/controls.

The cooling coil (CC) of the OAU regulates the dewpoint of this “outdoor” airflow and/or lowers the dry-bulb temperature, while the internal electric reheat element independently regulates its temperature. The steam spray humidifier (SSH) provides humidification capability in case ambient conditions require raising the dewpoint to an experiment’s specification instead of lowering it. The OAU, along with ductwork giving it an inlet and an outlet to the real outdoors, creates a circulating flow of treated air whose flowrate can be maintained independent from the amount of air drawn in by the AHUs. The fan is connected to a variable frequency drive (VFD) that allows it to operate over a range of flow rates.

These components work together to provide the desired temperature and humidity at the outlet of the OAU as measured by T86 and RH351 (see Fig. 5), respectively. The specifications for each component are given in Table 1 and Fig. 6 is a picture of the OAU.

Table 1. Specifications for the components in the OAU.

Component	Description	Value
Cooling coil	Refrigerant	R410A
	Total capacity	68 kW (20 tons)
Electric heater	Capacity	60 kW
	SSR controller	(0 to 10) V
Steam spray humidifier	Steam pressure	34.5 kPa (15 psig)
	Steam rate	30 kg/h (67 lbm/h)
	Steam rate control via V2	(2 to 10) V
Fan	Maximum airflow	4757 m ³ /h (2800 cfm)
	Maximum speed	163 rad/s (1558 rpm)
	Total static pressure	708 Pa (2.8 inH ₂ O)

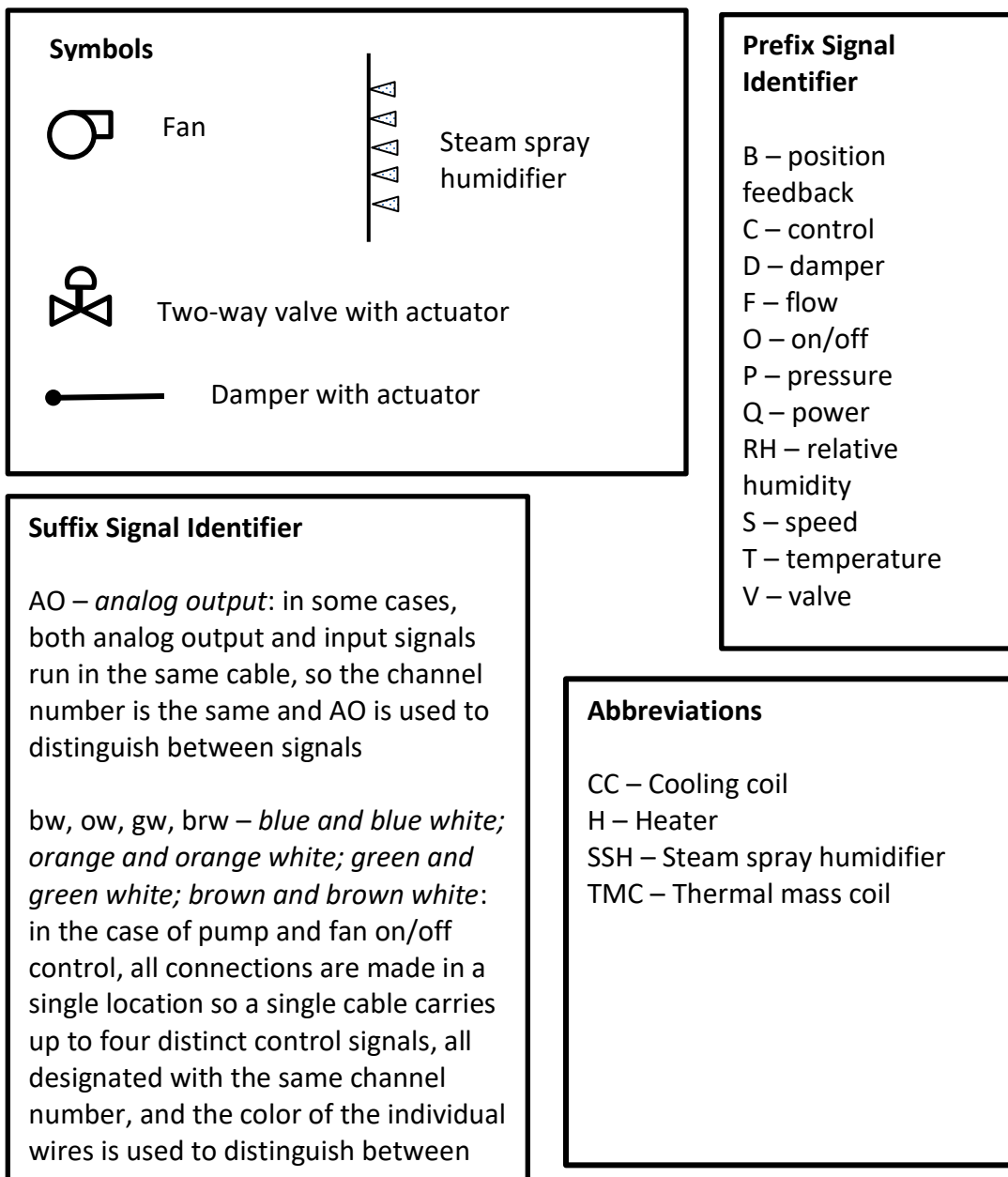


Fig. 4. Legend for the component schematics.

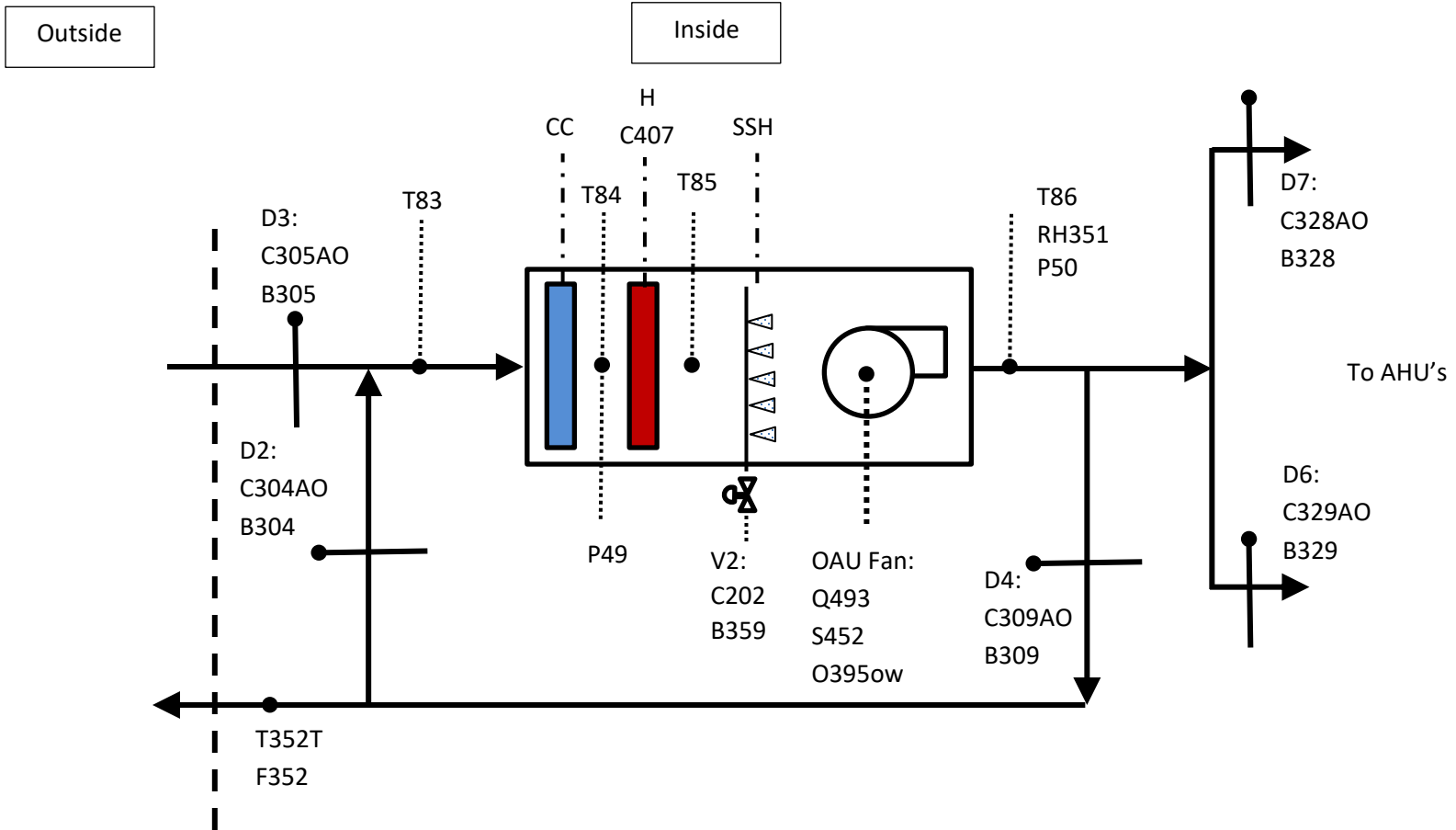


Fig. 5. Outdoor air unit (OAU).



Fig. 6. Picture of the OAU. Air is drawn in from the lower left, exits the OAU on the upper left of the unit, and goes to the AHUs at the right (not shown).

2.3. Air Handling Units

There are two identical AHUs, shown in Fig. 7, each nominally serving two zones. Specifications for the components in the AHUs are given in Table 2. Their arrangement follows an HVAC system design practice described in [4] as “single-duct VAV with reheat,” commonly applied to commercial and institutional buildings. The first element of the AHU is electric preheat, which prevents the CC from freezing if the “outside” air is too cold. The CC follows the heater. In the table the design numbers are based on a coolant consisting of 25 % PG by volume, but once the equipment was in the IBAL the PG percentage was increased to 30 %, which affects the heat transfer properties by a small amount. The fan is the last component in the AHU and operates from a VFD. Figure 8 is a picture of the two AHUs.

Table 2. Specifications for the components in the AHU.

Component	Description	Value
Electric heater	Capacity	9 kW
	Step controller	(0 to 10) V
Cooling coil	Refrigerant	25 % PG
	Total capacity	17.6 kW (5 tons)
	Refrigerant design flow	2 m ³ /h (9 gpm)
	Entering dry/wet bulb	26.7 °C/19.4 °C
	Leaving dry/wet bulb	12.8 °C/12.7 °C
	Entering PG	5.6 °C
Fan	Leaving PG	12.5 °C
	Maximum airflow	2379 m ³ /h (1400 cfm)
	Maximum speed	356 rad/s (3396 rpm)
	Total static pressure	970 Pa (3.893 inH ₂ O)

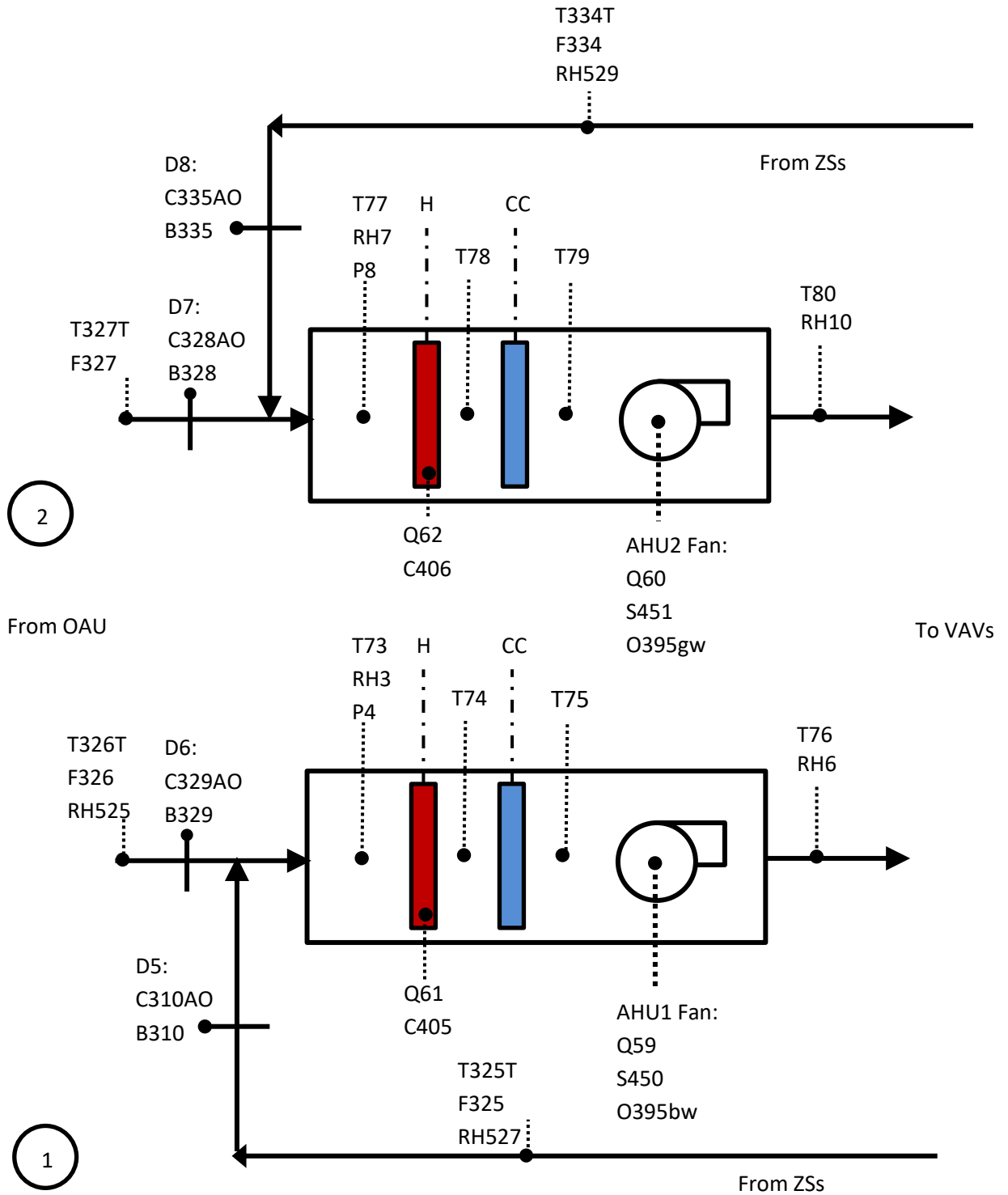


Fig. 7. Air Handling Units (AHUs). See Fig. 4 for the legend.



Fig. 8. AHU2 (top) and AHU1 (bottom). The OAU is on the upper mezzanine at the far left of the picture and the VAVs, not shown, are to the right.

2.4. Variable Air Volume Units

A VAV unit modulates the flowrate of air from an AHU to match the thermal load in the zone it supplies. Having the VAV unit include a “reheat” device allows the same AHU to serve multiple zones even if those zones have very different thermal loads. The IBAL contains four identical VAVs. Each contains a damper for flowrate control and an electric heater for reheat. In a typical control algorithm, the damper is given primary control over zone conditions. If the zone is too cold, the damper will close to reduce the flow of air entering the zone, but if the zone is also “occupied,” then ventilation (i.e., fresh air) standards set a lower limit on how much the damper can close. If the damper reaches that limit and the zone is still too cold, the electric heater can be used to reheat the air. The electric heater has a 2 kW capacity. Figure 9 shows the VAVs and the sensors associated with them and Fig. 10 is a picture of the VAVs.

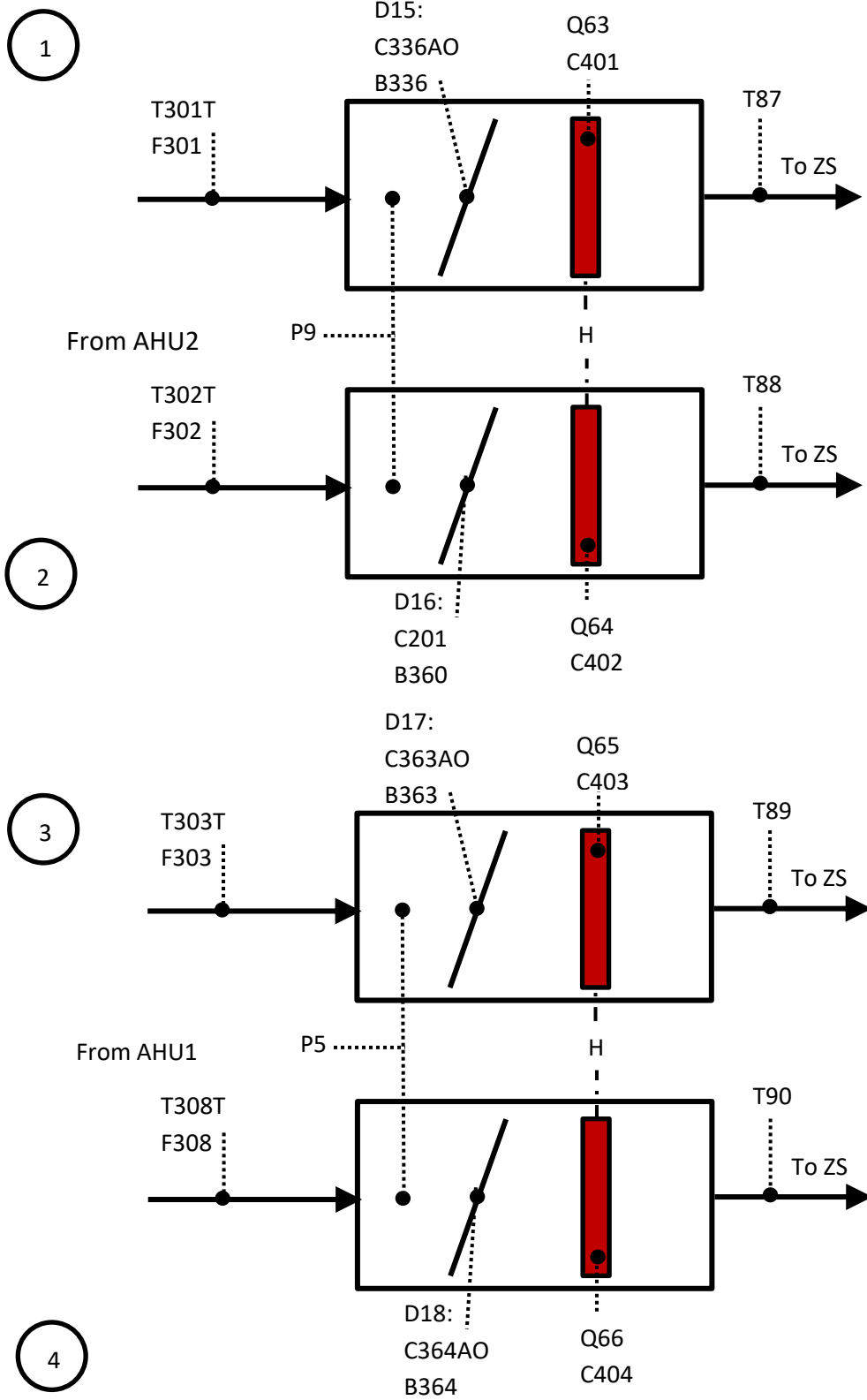


Fig. 9. Variable air volume boxes (VAV). See Fig. 4 for the legend.



Fig. 10. Picture of the VAVs. The AHUs are to the left and the ZSs are to the right.

2.5. Zone Simulators

Building HVAC systems are designed based on the expected building loads. The IBAL does not include an actual building or rooms due to space constraints, but zone simulators (ZSs) were designed to provide a load to be met by the HVAC system. There are four ZSs, each containing an electric heater, a SSH, a CC, and a TMC. The electric heater provides the sensible cooling load, the SSH supplies the latent cooling load, the CC provides a heating load, and the TMC provides a source of thermal mass. The focus of the IBAL is to study control systems to meet cooling loads with the underlying belief that the developed methodologies can be adapted to meet heating loads, so the CC is not currently used. Figure 11 is a schematic of the ZSs.

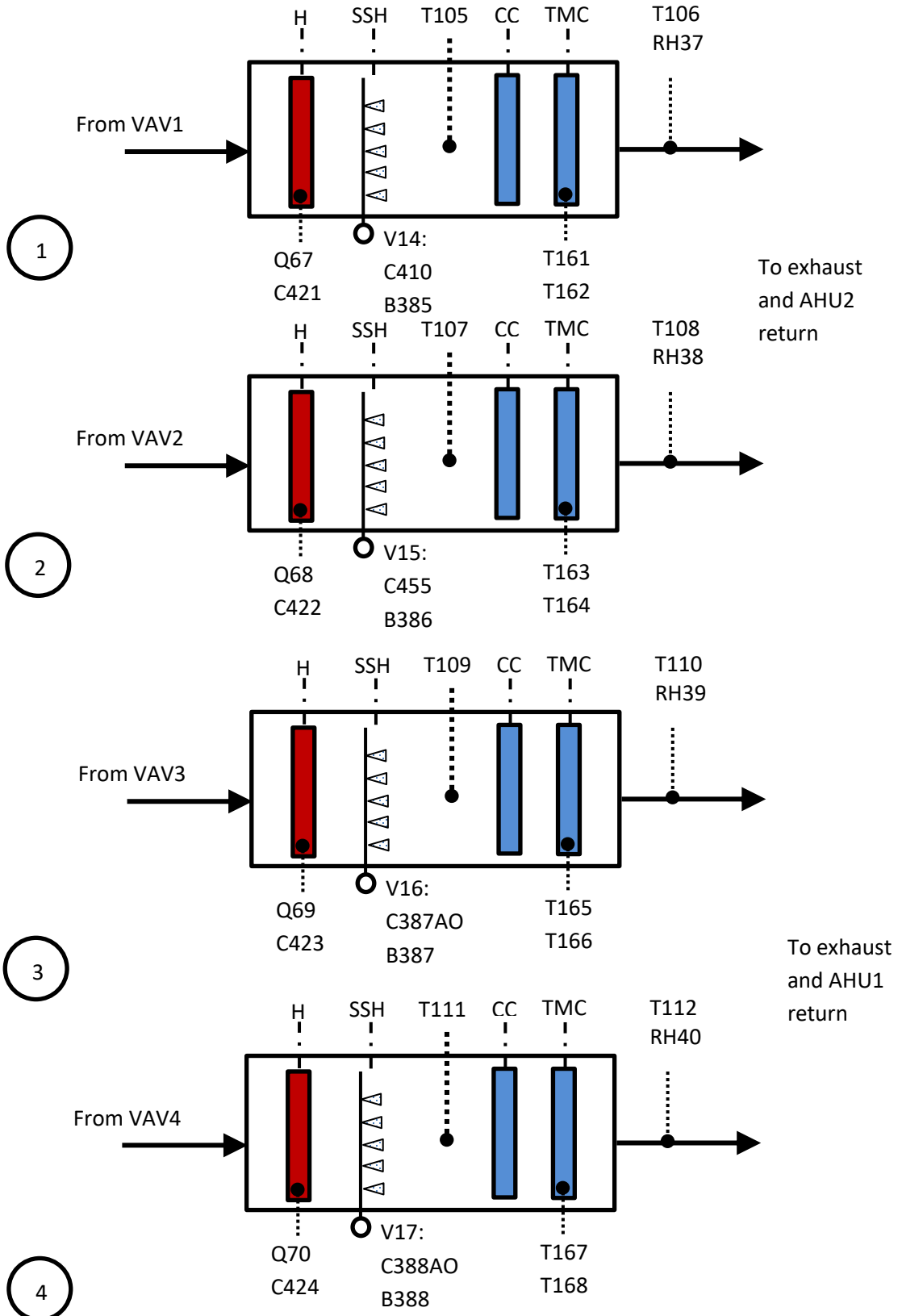


Fig. 11. Zone simulators (ZS). See Fig. 4 for the legend.

The four ZSs are stacked one above the other at one end of the mezzanine as shown in Fig. 12. Beginning at the far left and moving right are an electric heater, SSH, an access door, a CC, and a TMC (copper pipe runs from the TMC to a water tank). The zone temperature and humidity are measured at the outlet of the ZS.



Fig. 12. Picture of the four ZSs. The VAVs are at the left.

Each ZS was designed to represent a 65 m² (700 ft²) room in an office building and the equipment within the ZS was sized to provide the loads defined by each of two cases: (1) open office space and (2) conference room. The magnitude of the loads in both cases are based on the tables in the ASHRAE Handbook of Fundamentals [5]. For Case 1, there are six occupants, each performing office work. The room has a 32.5 m² (350 ft²) exterior wall with 7 m² (75 ft²) of glass facing southwest, and the magnitude of the heat gain through the envelope is based on conditions in Maryland. A summary of the loads for this zone is provided in Table 3. The sensible load is provided by the electric heater and the latent load is provided by the SSH.

Table 3. Loads for Case 1: open office space.

Source	Type of Load	Load	Total Load
Person	Sensible heat	72 W (245 BTU/h)	430 W (1470 BTU/h)
	Latent heat load	60 W (205 BTU/h)	360.5 W (1230 BTU/h)
Equipment	Workstation	175 W (597 BTU/h)	1050 W (3583 BTU/h)
Lighting	Lighting	11.8 W/m ² (1.1 W/ft ²)	770 W (2627 BTU/h)
Envelope	Heat gain	2344 W (8000 BTU/h)	2344 W (8000 BTU/h)
		Total	4955 W (16,910 BTU/h)

For Case 2 (see Table 4) there are 18 people performing office work in the conference room. There is one projector and one workstation and the envelope is the same as in Case 1.

Table 4. Loads for Case 2: conference room.

Source	Type of Load	Load	Total Load
Person	Sensible heat	72 W (245 BTU/h)	1292 W (4410 BTU/h)
	Latent heat load	60 W (205 BTU/h)	1081 W (3690 BTU/h)
Equipment	Workstation + projector	500 W (1706 BTU/h)	500 W (1706 BTU/h)
Lighting	Lighting	11.8 W/m ² (1.1 W/ft ²)	770 W (2627 BTU/h)
Envelope	Heat gain	2344 W (8000 BTU/h)	2344 W (8000 BTU/h)
		Total	5987 W (20,433 BTU/h)

The electric heater and SSH were selected to meet either of these two cases as a minimum, but the ZS operation will not be limited to these scenarios. Table 5 shows the specifications for the key components in the ZS and the required level of operation for each of the cases.

Table 5. Specifications for the components in the ZSs.

Component	Description	Value	Case 1	Case 2
Electric heater	Capacity ¹ SCR controller	5 kW (0 to 10) V	4.59 kW	4.9 kW
	Minimum airflow	187 m ³ /h (110 cfm)		
Steam spray humidifier	Steam pressure	34.5 kPa (15 psig)		
	Steam rate	1.8 kg/h (4 lbm/h)	0.6 kg/h (1.25 lbm/h)	1.8 kg/h (4 lbm/h)

¹Silicon-controlled rectifier

The electric heater and SSH provide a means to simulate the cooling loads in a zone, but a real zone also has thermal mass that acts to damp out changes in the temperature of the zone. For example, in a real room if an additional person (additional load) enters the room, the room temperature does not immediately increase. If there is no equivalent thermal mass in the ZS, an increase in the heater level will lead to an immediate change in temperature. The TMC is designed to provide the ZS with a means to damp out temperature changes. It was sized to mimic the effect of adding an occupant and workstation to the zone such that the temperature of the room would rise by 0.56 °C (1 °F) in 120 s. The volume of water required to achieve this effect is calculated as shown in Eq. (1). To achieve the desired effect, a water volume of 13 L (3.35 gal) is required.

$$\begin{aligned} \text{Volume [m}^3\text{]} &= \frac{Q \text{ [kW]} t \text{ [s]}}{c_p \text{ [kJ/kg - K]} \Delta T \text{ [K]} \rho \text{ [kg/m}^3\text{]}} \\ Q &= 72 + 175 = 247 \text{ W} \\ t &= 120 \text{ s} \\ c_p &= 4.18 \text{ kJ/kg - K} \\ \Delta T &= 0.56 \text{ K} \\ \rho &= 998 \text{ kg/m}^3 \end{aligned} \tag{1}$$

Rather than just placing a container of water in each ZS that will heat up over time, fluid circulates through the TMC so that at any given moment there is a volume of water in the TMC, but since it is not stagnant it has an opportunity to release heat outside of the ZS. Each TMC is independently supplied by a 76 L (20-gallon) water tank with a dedicated circulating pump. The flow rate of the water through the coil will be adjusted to achieve the desired effect. Figure 13 shows the water tanks and circulating pumps that supply the TMC.



Fig. 13. The black tanks hold water for the thermal mass coils in the zone simulators. Above the tanks are the red circulating pumps that move the water through the TMCs. The flow rate is determined by manually setting a valve.

The four zone simulators together can generate a sensible load of 20 kW (5.7 ton) and a latent load of approximately 4.3 kW (1.2 ton), for a total load of 24 kW (6.9 ton).

2.6. Exhaust Fans

The IBAL contains two identical exhaust fans that push air outside. Table 6 contains the specifications for the fans.

Table 6. Specifications for the exhaust fans.

Component	Description	Value
Fan	Maximum airflow	2379 m ³ /h (1400 cfm)
	Maximum speed	226 rad/s (2156 rpm)
	Total static pressure	249 Pa (1 inH ₂ O)

2.7. Data Collection and Operation

The data acquisition system (DAQ) was described in detail in Technical Note 1933, Sec. 4 [3]. The air system uses the same equipment and control software approach.

3. Measurement Uncertainty Calculations

This section provides an overview of the calibration curve fits for the air pressure and relative humidity (RH) measurements. Sections 3.1 and 3.2 are reproduced, and updated as appropriate, from Ref. [3]. The Appendix contains detailed calculations; the results presented in this section are shown with fewer significant digits.

3.1. Overview

According to Taylor and Kuyatt [6], uncertainty is categorized as one of two types, Type A or Type B. Type A uncertainties are determined from a statistical evaluation of data, such as calculating standard deviation from a series of independent measurements. Uncertainty calculated from calibration data is an example of Type A. Type B uncertainties are based on scientific judgement and prior data, such as manufacturer specifications. When there is more than one source of uncertainty, they are summed in quadrature as shown in Eq. (2).

$$u_{total} = \sqrt{u_1^2 + u_2^2 + \dots + u_n^2} \quad (2)$$

Table 7 contains the measurement uncertainties of the hardware in the DAQ. These values are included in the total uncertainty calculation. *AI uncertainty* is the uncertainty of an analog input channel and *AO uncertainty* is the uncertainty of an analog output channel.

Table 7. Uncertainties of temperature, voltage, and current measurements of DAQ hardware.

Card	AI uncertainty	Units	AO uncertainty	Units
4357	0.126	°C		
4300	0.002 460	V		
6238	0.000 018 8	A	0.000 052 3	A
6363	0.001 66	V	0.001 89	V
6704			0.001 07	V
			0.000 000 448	A
6345	0.001 520	V	0.001 89	V

3.2. Uncertainty of Calibration Curve Fit

This section contains the equations used to calculate the uncertainty of the curve fit derived from calibration data that relates the measured voltage signal to the engineering units of the sensor. For example, the pressure transducers in the air system output a current signal that is converted to voltage at the DAQ by dropping it across a 249 Ω resistor, the voltage is measured by card 4300, and then converted to inH₂O. The relationship between the measured signal and engineering units is linear. During calibration, pressure or relative humidity is the dependent y variable, while voltage is the independent x variable. Equation (3) shows the relationship between the dependent and independent variables, where the slope a_1 and intercept a_0 are found from the calibration data as shown in Eqs. (5) and (6) [7]. In this case the dependent variable is \hat{y} , which is the result of the curve fit. The standard error of the calibration is determined from the fit by calculating the residual y_r between the fit \hat{y} and the measured y as shown in Eqs. (3) and (4).

$$\hat{y} = a_1 x + a_0 \quad (3)$$

$$y_r = y - \hat{y} \quad (4)$$

$$a_1 = \frac{S_{xy}}{S_{xx}} \quad (5)$$

$$a_0 = \bar{y} - a_1 \bar{x} \quad (6)$$

$$\bar{x} = \frac{\sum_{i=1}^n x_i}{n} \quad (7)$$

$$S_{xy} = \sum x_i y_i - \frac{\sum x_i \sum y_i}{n} = \sum (x_i - \bar{x})(y_i - \bar{y}) \quad (8)$$

$$S_{xx} = \sum x_i^2 - \frac{(\sum x_i)^2}{n} = \sum (x_i - \bar{x})^2 \quad (9)$$

The standard error, se , is calculated by dividing the sum of the squares of the residuals, $SSResid$, by the number of degrees of freedom, ν , and taking the square root. The expanded standard error, se_e , which is the 95 % confidence interval, is calculated by multiplying the se by the t statistic that corresponds to the degrees of freedom. See Eqs. (10) through (13). This final error is the calibration uncertainty.

$$SSResid = \sum_{i=1}^n y_{r_i}^2 \quad (10)$$

$$\nu = n - 2 \quad (11)$$

$$se = \sqrt{\frac{SSResid}{\nu}} \quad (12)$$

$$se_e = t \cdot se \quad (13)$$

The total uncertainty is calculated by adding additional uncertainties, such as the DAQ measurement uncertainty from Table 7 and the uncertainty in the calibration standard, as shown in Eq. (14). The DAQ measurement uncertainty is scaled to the same units as the other uncertainties by multiplying it by the slope a_1 .

$$u_{total} = \sqrt{se_e^2 + u_{other}^2} \quad (14)$$

3.3. Pressure Transducers

In the IBAL duct air pressure is measured in ten locations using capacitance sensors. The sensors output a current signal (mA) that is proportional to the pressure. That current is passed through a 249 Ω resistor and the voltage across this resistor is read by card 4300. The pressure sensors have two uses: 1) monitor fan performance and 2) provide a controller input. In the former case, a pressure measurement is made both upstream and downstream of a fan to monitor the static pressure generated by the fan. Changes in that measurement over time can indicate if there are problems with a fan. In the latter case, the pressure measurement is used by the control system to change fan speed in response to a change in the duct static pressure. For example, if a VAV damper closes because the zone needs less airflow, the duct static pressure will increase, and the control system can decrease the fan speed so that it delivers less air to the VAV. This type of operation decreases the fan energy consumption. In both cases, the absolute accuracy of the measurement is not the key, the accuracy of the measurement of *changes* in the pressure from one time to another is the key.

The calibration was performed using a precision pressure controller with a (0 to 2491) Pa ((0 to 10) inH₂O) pressure regulator. The uncertainty of the reference standard is 74.7 Pa (0.003 inH₂O). The calibration does not address the pitot tube-pressure transducer system, but just the pressure transducer accuracy. Figure 14 shows the calibration setup and Table 8 shows the results.



Fig. 14. Picture of the air pressure calibration setup. The precision pressure controller is at the far left and two pressure transducers (the gray boxes) are visible.

For channels whose range includes negative pressures, the calibration only included positive values because the transducer is linear with pressure and a vacuum supply was unavailable for the negative range. The other channels were calibrated over the full positive range. In all cases the order in which calibration pressures were applied to the transducer was randomly determined. At least 40 data points were acquired at each pressure setting. Note that for channel 50 there is a third calibration term. This is a quadratic term and when the calibration fit was calculated that term was found to be significant.

Table 8. Air pressure transducer uncertainty results.

Channel Number	Range [Pa] (inH ₂ O)	a ₀ [Pa] (inH ₂ O)	a ₁ [Pa/V] (inH ₂ O/V)	a ₂ [Pa/V ²] (inH ₂ O/V ²)	u _{total} [Pa] (inH ₂ O)
4	0 to 1245 (0 to 5)	-946.5 (-3.8)	313.9 (1.26)		3.99 (0.016)
5	-933.15 to 933.15 (-3.75 to 3.75)	-480.7 (-1.93)	495.7 (1.99)		1.89 (0.0076)
8	0 to 1245 (0 to 5)	-941.6 (-3.79)	313.9 (1.26)		3.74 (0.015)
9	-933.15 to 933.15 (-3.75 to 3.75)	-503.2 (-2.02)	488.2 (1.96)		2.99 (0.012)
13	0 to 249 (0 to 1)	-67.3 (-0.27)	62.3 (0.25)		0.80 (0.0033)

Channel Number	Range [Pa] (inH ₂ O)	a ₀ [Pa] (inH ₂ O)	a ₁ [Pa/V] (inH ₂ O/V)	a ₂ [Pa/V ²] (inH ₂ O/ V ²)	u _{total} [Pa] (inH ₂ O)
14	0 to 249 (0 to 1)	-62.3 (-0.25)	62.3 (0.25)		0.82 (0.0033)
16	0 to 249 (0 to 1)	-64.8 (-0.26)	62.3 (0.25)		0.85 (0.0034)
17	0 to 249 (0 to 1)	-69.7 (-0.28)	62.3 (0.25)		1 (0.004)
49	0 to 1245 (0 to 5)	-934.1 (-3.76)	313.9 (1.26)		2.74 (0.011)
50	0 to 1245 (0 to 5)	-308.9 (-1.24)	313.9 (1.26)	1.046 (-0.0042)	1.89 (0.0076)

3.4. Airflow Sensors

The airflow sensors use thermal dispersion technology to measure both airflow and temperature. The sensor is factory calibrated to a NIST-traceable standard and the manufacturer recommends not calibrating the system in-situ, therefore, the manufacturer specified uncertainty and DAQ card uncertainty, shown in Table 9, were used to estimate the total uncertainty. The airflow sensors output two (4 to 20) mA signals that are converted to voltage by passing each of them through a 249 Ω resistor and then reading the voltage across the resistor using card 6363.

Subsequent operations have, however, shown that this uncertainty is too low. This conclusion was reached by looking at an energy balance on the cooling coils in the AHUs. In some tests there was an energy imbalance between the hydronic and air sides of the cooling coil of as much as 30 %. This imbalance was the result of several factors, but the most significant was the inaccuracy of the airflow measurements. Further work will be conducted to determine the uncertainty of the airflow measurements more precisely, but at this time the value is set as 10 % of reading based on the energy balance investigations.

Table 9. Measurement uncertainty of airflow sensors.

Measurement	Manufacturer Uncertainty	Card Uncertainty
Airflow	± 2 % of reading	0.001 66 V
Temperature	± 0.08 °C (0.15 °F)	0.001 66 V

The conversions from voltage to engineering units for the various airflow sensors are provided in Table 10.

Table 10. Conversion factors for airflow sensors.

Channel Number	a ₀	a ₁
301	-644 m ³ /h (-379.03 cfm)	644.7 m ³ /h-V (379.45 cfm/V)
302	-643.9 m ³ /h (-378.96 cfm)	643.9 m ³ /h-V (378.96 cfm/V)
303	-644 m ³ /h (-379.03 cfm)	644 m ³ /h-V (379.06 cfm/V)
306	-855.2 m ³ /h (-503.34 cfm)	858.8 m ³ /h-V (505.47 cfm/V)
307	-855.2 m ³ /h (-503.34 cfm)	858.8 m ³ /h-V (505.47 cfm/V)
308	-643.9 m ³ /h (-378.96 cfm)	643.8 m ³ /h-V (378.9 cfm/V)
325	-855.2 m ³ /h (-503.34 cfm)	858.8 m ³ /h-V (505.47 cfm/V)

Channel Number	a_0	a_1
326	-855.2 m ³ /h (-503.34 cfm)	858.8 m ³ /h-V (505.47 cfm/V)
327	-855.2 m ³ /h (-503.34 cfm)	858.8 m ³ /h-V (505.47 cfm/V)
334	-855.2 m ³ /h (-503.34 cfm)	858.8 m ³ /h-V (505.47 cfm/V)
352	-1512.9 m ³ /h (-889.95 cfm)	756.3 m ³ /h-V (444.9 cfm/V)
301T	-7.03 °C (-12.65 °F)	12.64 °C/V (22.75 °F/V)
302T	-7.03 °C (-12.65 °F)	12.64 °C/V (22.75 °F/V)
303T	-7.03 °C (-12.65 °F)	12.64 °C/V (22.75 °F/V)
306T	-7.03 °C (-12.65 °F)	12.64 °C/V (22.75 °F/V)
307T	-7.03 °C (-12.65 °F)	12.64 °C/V (22.75 °F/V)
308T	-7.03 °C (-12.65 °F)	12.64 °C/V (22.75 °F/V)
325T	-7.03 °C (-12.65 °F)	12.64 °C/V (22.75 °F/V)
326T	-8.41 °C (-15.13 °F)	14.05 °C/V (25.29 °F/V)
327T	-8.41 °C (-15.13 °F)	14.05 °C/V (25.29 °F/V)
334T	-7.03 °C (-12.65 °F)	12.64 °C/V (22.75 °F/V)
352T	-15.37 °C (-27.66 °F)	7.8 °C/V (13.98 °F/V)

3.5. Relative Humidity Sensors

The RH sensors use a capacitive sensing element to measure RH. The sensors output a (4 to 20) mA signal that is converted to voltage at the DAQ across a 249 Ω resistor. The humidity sensors were calibrated in-situ using the Vaisala MI70-HMP76¹ humidity and temperature probe, which has an uncertainty of 1 % relative humidity. This uncertainty is much lower than the uncertainty of the calibration fit. The results of the calibration are given in Table 11.

Table 11. Measurement uncertainty and calibration fit for RH sensors.

Channel Number	a_0 [%]	a_1 [%/V]	u_{total} [%]
3	-25.27	25.63	1.28
6	-24.53	24.91	0.72
7	-26.8	26.05	1.12
10	-24.51	25.35	0.89
37	-12.68	21.24	1.41
38	-24.49	25.49	1.05
39	-24.55	25.4	0.69
40	-24.31	25.31	0.54
51	-25	25	3
351	-25.56	25.25	0.64
497	-25	12.5	2
525	-24.48	12.68	0.3
527	-24.43	12.65	0.16
529	-24.66	12.73	0.14

¹ Certain equipment, instruments, software, or materials, commercial or non-commercial, are identified in this paper in order to specify the experimental procedure adequately. Such identification does not imply recommendation or endorsement of any product or service by NIST, nor does it imply that the materials or equipment identified are necessarily the best available for the purpose.

4. Summary and Future Work

This paper described the design of the air system, including the equipment and measurement uncertainty of some of the key instrumentation. Additional measurement uncertainty calculations will be detailed in a future technical note. The schematics showed the location of measurements and the channel numbers corresponding to those measurements. The IBAL as it stands to date has now been described in full.

Work will continue to develop the software to automate the operation of the IBAL. Additional publications will detail the control and characteristics of subsystems such as the OAU. The major focus will be on the development of intelligent control algorithms for the operation of the facility.

5. References

- [1] US Energy Information Administration, "U.S. energy flow, 2017," 2017. [Online]. Available: https://www.eia.gov/totalenergy/data/monthly/pdf/flow/total_energy.pdf. [Accessed: 06-Sep-2018].
- [2] G. E. Kelly and S. T. Bushby, "Are intelligent agents the key to optimizing building HVAC system performance?," *HVAC R Res.*, vol. 18, no. 4, pp. 750–759, 2012.
- [3] A. J. Pertzborn, "NIST Technical Note 1933: Intelligent Building Agents Laboratory : Hydronic System Design," 2016.
- [4] H. G. Lorsch, *Air-Conditioning Systems Design Manual*. American Society of Heating, Refrigerating and Air-Conditioning Engineers, 1993.
- [5] ASHRAE, *ASHRAE handbook of fundamentals*. Atlanta: Atlanta: American Society of Heating, Air-Conditioning and Refrigeration Engineers, Inc., 2009.
- [6] B. N. Taylor and C. E. Kuyatt, "NIST Technical Note 1297: Guidelines for Evaluating and Expressing the Uncertainty of NIST Measurement Results," 1994.
- [7] J. Devore and N. Farnum, *Applied Statistics for Engineers and Scientists*, 2nd ed. Belmont, CA: Thomson Brooks/Cole, 2005.
- [8] NIST, "HVAC& R Equipment Environmental Chambers | NIST." [Online]. Available: <https://www.nist.gov/laboratories/tools-instruments/hvacr-equipment-environmental-chambers>. [Accessed: 13-Sep-2018].

Appendix A. List of Symbols, Abbreviations, and Acronyms

<i>a</i>	calibration constant
<i>b</i>	intercept
<i>m</i>	slope
<i>n</i>	number of data points
<i>s</i>	standard deviation
<i>se</i>	standard error
<i>t</i>	value of the Student t-test
<i>u</i>	uncertainty
<i>x</i>	independent variable
<i>y</i>	dependent variable
AHU	air-handling unit
AI	analog input
AO	analog output
BACnet	building automation and control networks
CC	cooling coil
EXF	exhaust fan
IBAL	Intelligent Building Agents Laboratory
OAU	outdoor air unit
P/N	part number
RH	relative humidity
S	value used in calculating a linear curve fit
SCR	silicon-controlled rectifier
S/N	serial number
SS	sum of squares
SSH	steam spray humidifier
<i>SSResid</i>	sum of the square of residuals
TMC	thermal mass coil
VAV	variable air volume
ZS	zone simulator

Subscripts

0	term in the calibration curve fit
1	term in the calibration curve fit
d	downstream
e	expanded
r	residual
total	calculated from all results
u	upstream
xx	term using only independent variable

xy term using the independent and dependent variables

Other symbols

- \bar{x} mean of "x"
- \hat{x} value of "x" from a curve fit
- ν degrees of freedom

Appendix B. Sensor Information²

This Appendix contains a list of the sensors in the air system with part numbers (Table 12) and data for the uncertainty calculations (Table 13 and Table 14). Sensors that were not calibrated at NIST, but rather use the manufacturer uncertainty and conversion from voltage to engineering units, are not included in these tables.

Table 12. Summary of sensors in the air system in the IBAL.

Sensor	Channel Number	P/N	S/N
Pressure	4	Mamac PR274-R3-MA	
	5	Mamac PR274-R4-MA	
	8	Mamac PR274-R3-MA	
	9	Mamac PR274-R4-MA	
	13	Mamac PR274-R2-MA	
	14	Mamac PR274-R2-MA	
	16	Mamac PR274-R2-MA	
	17	Mamac PR274-R2-MA	
	49	Mamac PR274-R2-MA	
50	Mamac PR274-R2-MA		
Relative Humidity	3	ACI A/RH2-100-R2	
	6	ACI A/RH2-100-R2	
	7	ACI A/RH2-100-R2	
	10	ACI A/RH2-100-R2	
	37	HMD60U	M2350314
	38	ACI A/RH2-100-R2	
	39	ACI A/RH2-100-R2	
	40	ACI A/RH2-100-R2	
	51	ACI A/RH2-100-R2	
	349		50377564
	351	RHP-2R1D-NIST	M08783
	497	HMD62	M2350313
	525	HMD62	R2340291
527	HMD62	R2340290	
529	HMD62	R2340288	
Airflow and Temperature	301, 301T	Ebtron GTC116-P+1/2	708322
	302, 302T	Ebtron GTC116-P+1/2	708558
	303, 303T	Ebtron GTC116-P+1/2	708564
	306, 306T	Ebtron GTC116-P+1/2	708432
	307, 307T	Ebtron GTC116-P+1/2	708422
	308, 308T	Ebtron GTC116-P+1/2	708554
	325, 325T	Ebtron GTC116-P+1/2	708439
	326, 326T	Ebtron GTC116-P+1/2	707957
	327, 327T	Ebtron GTC116-P+1/2	708382
	334, 334T	Ebtron GTC116-P+1/2	708329
352, 352T	Ebtron GTC116-P+1/2	50217663	

² Certain equipment, instruments, software, or materials, commercial or non-commercial, are identified in this paper in order to specify the experimental procedure adequately. Such identification does not imply recommendation or endorsement of any product or service by NIST, nor does it imply that the materials or equipment identified are necessarily the best available for the purpose.

Table 13. Calibration data for pressure transducers.

Channel Number	n	\bar{x} [V]	\bar{y} [inH ₂ O]	S_{xy} [inH ₂ O -V]	S_{xx} [V ²]	SSResid [inH ₂ O ²]	ν	se [inH ₂ O]	t	a_0 [inH ₂ O]	a_1 [inH ₂ O /V]	a_2 [inH ₂ O /V ²]	u_{total} [inH ₂ O]
4	10	3.87	1.07	2.72	2.16	0.00035	8	0.007	2.306	-3.804	1.261		0.0158
5	13	2.55	3.13	32.88	16.53	0.00006	11	0.002	2.201	-1.935	1.989		0.0076
8	10	3.85	1.07	2.72	2.15	0.00032	8	0.006	2.306	-3.787	1.263		0.0153
9	13	2.63	3.13	33.30	16.96	0.00026	11	0.005	2.201	-2.025	1.963		0.0122
13	11	3.06	0.50	4.37	17.35	0.00000	9	0.000	2.262	-0.269	0.252		0.0033
14	11	3.01	0.50	4.40	17.59	3.85	9	0.654	2.262	-0.252	0.250		0.0033
16	11	3.03	0.50	4.38	17.46	0.00000	9	0.001	2.262	-0.260	0.251		0.0034
17	11	3.11	0.50	4.39	17.51	3.85	9	0.654	2.262	-0.280	0.251		0.0040
49	10	3.94	1.20	5.24	4.16	0.00017	8	0.005	2.306	-3.759	1.258		0.0115
50	15						12	0.003	2.179	-1.236	1.261	-0.004	0.0076

Table 14. Calibration data for relative humidity sensors.

Channel Number	n	\bar{x} [V]	\bar{y} [%]	S_{xy} [%-V]	S_{xx} [V ²]	SSResid [% ²]	ν	se [%]	t	a_0 [%]	a_1 [%/V]	U_{total} [%]
3	8	2.65	42.66	143.04	5.58	1.63	6	0.52	2.45	-25.27	25.63	1.28
6	7	3.22	55.8	55.94	2.25	0.38	5	0.28	2.57	-24.53	24.91	0.72
7	9	3.44	62.85	175.45	6.73	1.55	7	0.47	2.36	-26.8	26.05	1.12
10	6	3.35	60.41	106.85	4.22	0.41	4	0.32	2.78	-24.51	25.35	0.89
37	7	3.36	58.8	7.94	0.37	1.5	5	0.55	2.57	-12.68	21.24	1.41
38	10	3.01	52.15	167.0	6.55	1.65	8	0.45	2.31	-24.49	25.49	1.05
39	8	2.86	49.97	90.68	3.57	0.48	6	0.8	2.45	-24.55	25.4	0.69
40	6	3.06	53.1	83.97	3.32	0.15	4	0.19	2.78	-24.31	25.31	0.54
525	7	6.34	55.86	96.6	7.62	0.066	5	0.11	2.57	-24.48	12.68	0.3
527	8	6.76	61.1	355.29	28.08	0.024	6	0.063	2.45	-24.43	12.65	0.16
529	10	5.99	51.66	299.02	23.49	0.027	8	0.058	2.31	-24.66	12.73	0.14

Appendix C. Change Log

Date	Type of Edit	Change	Location
01/05/2024	Author update	Added Glen Glaeser as an author	Title page
01/05/2024	Data change	Updated calibration information and added new sensors to the lists	Appendix B, Table 11, Table 8, Table 10
01/05/2024	Update equations	Updated the text describing the calculation of measurement uncertainty to reflect the current approach	Section 3.2
01/05/2024	Update text	Updated the text describing calibration procedures	Section 3.5
01/05/2024	Update text	Updated the section about the uncertainty of airflow measurements	Section 3.4
01/05/2024	Update figures	Added new sensors to Figures 5 and 7	Figure 5, Figure 7
01/05/2024	Update text	Updated conclusion based on current state of the work	Section 4